Experimental Assessment of Structural Differences between Amorphous and Amorphized Matter

Thomas Höche*

Leibniz-Institut für Oberflächenmodifizierung e.V., Permoserstrasse 15, D-04318 Leipzig, Germany

Frank Schrempel

Institut für Festkörperphysik, Friedrich-Schiller-Universität Jena, Max-Wien-Platz 1, D-07743 Jena, Germany

Michael Grodzicki

Institut für Mineralogie, Universität Salzburg, Hellbrunner Strasse 34, A-5020 Salzburg, Austria

Peter A. van Aken

Max-Planck-Institut für Metallforschung, Heisenbergstrasse 3, D-70569 Stuttgart, Germany

Frank Heyroth

Interdisziplinäres Zentrum für Materialwissenschaften, Martin-Luther-Universität Halle-Wittenberg, Hoher Weg 8, D-06120 Halle, Germany

Received March 16, 2006. Revised Manuscript Received July 17, 2006

The atomic structure of amorphous matter as well as its relation to properties constitute key materials-science challenges of tomorrow. High-resolution transition-metal $L_{2,3}$ electron energy-loss near-edge structure spectroscopy in the transmission electron microscope at a barium titanium silicate glass and its amorphized counterpart, prepared by ion irradiation of a single crystal of identical composition, is shown to be capable of distinguishing different cation coordination. The introduced methodology is able to separate polyamorphous phases at nanometer spatial resolution and hence of greatest relevance for the experimental assessment of structural preconditions for sintering of ceramics and controlled devitrification of glasses.

Introduction

In-depth understanding of the structure−properties relationship of amorphous thin films (e.g., ultrathin gate oxides, ion-beam amorphized superficial layers, or nanometer-sized wetting layers at grain boundaries) becomes increasingly important for controlling device functions. In this respect, a technique capable of assessing valence and coordination of cations in conjunction with a high spatial resolution is mandatory. As exemplarily shown at Ti-$L_{2,3}$ and O-K electron energy-loss near-edge structures (ELNES)[1] of the crystalline TiO_2 polymorphs rutile and anatase, these requirements are excellently met by electron energy-loss spectroscopy (EELS) in the transmission electron microscope. While the coordination of a cation with oxygen sensitively influences the subsplitting of unoccupied energy levels and hence features in the ionization-edge near-edge structure,[2,3] valence changes result in chemical shifts.[4] For example, the reduction of Ti^{4+} toward Ti^{3+} is accompanied by a more effective shielding of the core potential causing a shift of the entire ionization edge toward lower energy losses.[5] The introduction of aberration-corrected transmission electron microscopes has made EELS studies utilizing sub-nanometer beams viable.[6,7] However, is this excellent tool applicable to discriminate structural variants in disordered matter?

In due course, we shall—on the basis of high-resolution electron energy-loss near-edge spectra—exemplarily prove that in amorphous barium titanium silicate ($2BaO-TiO_2-2SiO_2$) the coordination state of titanium not only can be clearly discerned but also differences between a glass and an amorphized single crystal of identical composition can be identified. We explicitly take advantage of the spatial resolution of ELNES spectroscopy, competing techniques including X-ray absorption spectroscopy and photoelectron spectroscopy are unable to achieve.

* Corresponding author. E-mail: thomas.hoeche@iom-leipzig.de

(1) Brydson, R.; Sauer, H.; Engel, W.; Thomas, J. M.; Zeitler, E.; Kosugi, N.; Kuroda, H. *J. Phys.: Condens. Matter* **1989**, *1*, 797−812.
(2) Höche, T.; van Aken, P. A.; Grodzicki, M.; Heyroth, F.; Keding, R.; Uecker, R. *Philos. Mag.* **2004**, *84*, 3117−3132.
(3) Höche, T.; Grodzicki, M.; Heyroth, F.; van Aken, P. A. *Phys. Rev. B* **2005**, 205111.
(4) Leapman, R. D.; Grunes, L. A.; Fejes, P. L. *Phys. Rev. B.* **1982**, *26*, 614−635.
(5) Höche, T.; Ohle, P.; Keding, R.; Rüssel, C.; van Aken, P. A.; Schneider, R.; Kleebe, H. J.; Wang, X. Q.; Jacobson, A. J.; Stemmer, S. *Philos. Mag.* **2003**, *83*, 165−178.
(6) Allen, L. J.; Findlay, S. D.; Lupini, A. R.; Oxley, M. P.; Pennycook, S. *J. Phys. Rev. Lett.* **2003**, *91*, 105503.
(7) Shibata, N.; Pennycook, S. J.; Gosnell, T. R.; Painter, G. S.; Shelton, W. A.; Becher, P. F. *Nature* **2004**, *428*, 730−733.

10.1021/cm060636a CCC: $33.50
Published on Web 09/29/2006

In EELS, the transition of bound core-state electrons into unoccupied states above Fermi but below continuum level cause characteristic energy losses in the energy distribution of the exciting electron beam. Particularly pronounced ELNES features are observed for 3d transition metals due to the excitation of bound 2p electrons into energetically narrow, unoccupied orbitals of primarily 3d character ($L_{2,3}$-ELNES). As shown earlier,[3,8] tetravalent titanium (Ti^{4+}) is almost ideally suited for an in-depth study of its coordination-dependent electronic structure since all 10 Ti(3d) states are unoccupied and titanium occurs in three different standard co-ordinations (tetrahedral, pentahedral, and octahedral) with oxygen. While for a free Ti^{4+} ion all 10 3d states are degenerated, a subdivision into five molecular orbitals occurs due to the crystal-field splitting in pentahedrally coordinated Ti^{4+}, and this splitting is characteristically reflected in the Ti-$L_{2,3}$ ELNES (cf. Figure 1 in ref 3).

Materials and Methods

While a clear and colorless $2BaO-TiO_2-2SiO_2$ glass was obtained by splat cooling a melt obtained from $BaCO_3$, TiO_2 (rutile), and SiO_2, a $Ba_2(TiO)(Si_2O_7)$ single crystal was grown by the Czochralski pulling technique. A polished fraction of the crystal was superficially amorphized by irradiation with 200 keV Ar^+ ions. Damage accumulation within the crystal was investigated by irradiation with ion fluences ranging between 1.0×10^{12} cm^{-2} and 1.5×10^{14} cm^{-2}. Rutherford backscattering spectrometry (RBS) in channeling configuration was applied using 2 MeV He^+ ions[9] in a double-beam chamber allowing stepwise ion implantation and subsequent RBS analysis. From RBS spectra, the minimum yield as a function of depth z, $\chi_{min}(z) = Y_{al}(z)/Y_{ra}(z)$, was determined with Y_{al} and Y_{ra} being the yield of the aligned and random spectra, respectively.

TEM foils were prepared from $2BaO-TiO_2-2SiO_2$ glass and single-crystalline $Ba_2(TiO)(Si_2O_7)$ by mechanical thinning followed by double-sided Ar^+ ion-beam etching at 2.5 kV acceleration voltage. Static charging of the foil was avoided by the deposition of an ultrathin carbon layer by usage of the CoatMaster kit for selective coating.[10,11] A cross-sectional TEM sample was prepared from the amorphized $Ba_2(TiO)(Si_2O_7)$ single-crystal perpendicular to the [001] direction following the route set out by Strecker et al.[12]

For EELS analytics, a dedicated scanning transmission electron microscope (VG HB501 UX) with a cold field emission gun and a parallel electron energy-loss spectrometer (Gatan Enfina 1000) was used. Routinely achieved energy resolution, defined as the full width at half-maximum of the zero-loss peak, amounts to $\Delta E_{fwhm} = 0.4$ eV, hence the spectral resolution at core-loss edges is on the order of 0.45 eV after averaging over approximately 20 spectra.[13] EEL spectra were acquired at an illumination convergence semi-angle of 14 mrad within a collection semi-angle of 13 mrad. Radiation damage was minimized by scanning the slightly defocused beam over an area of 50×50 nm^2. Approximately 20 spectra recorded at a dispersion of 0.05 eV/channel (each within 1 s) were energetically calibrated with sub-channel relative accuracy and averaged after correcting for dark current and noise as well as for channel-to-channel gain variations of the detector. The background was subtracted using an inverse power-law function and multiple-scattering and tailing effects of the zero-loss peak were deconvoluted by the Fourier ratio technique using the corresponding low-loss and zero-loss spectra, acquired consecutively to core-loss spectra from the same specimen region.[14] As described in detail earlier,[2] absolute energy calibration is as precise as two channels (i.e., 0.1 eV for the present 0.05 eV dispersion).

Theoretical Calculations. As detailed in a recent contribution,[3] a quantitative picture of the Ti(3d) orbitals in crystalline $Ba_2(TiO)(Si_2O_7)$ was developed by calculating the molecular orbital structure of appropriately sized model clusters within the local density approximation by the self-consistent charge (SCC) Xα method.[15]

Results and Discussion

The Ti-$L_{2,3}$ ELNES of $2BaO-TiO_2-2SiO_2$ glass (see Figure 1) can—according to ref 3—be interpreted as arising from the following average coordination distribution in the glass: $60 \pm 10\%$ $^{[5]}Ti^{4+}$, $20 \pm 10\%$ $^{[6]}Ti^{4+}$, and $20 \pm 10\%$ $^{[4]}Ti^{4+}$. Based on reference spectra of tetrahedrally, pentahedrally, and octahedrally coordinated Ti^{4+} also shown in Figure 1, the contribution of $^{[4]}Ti^{4+}$ is apparent from the shoulder at ~465 eV (B3), while octahedrally coordinated Ti^{4+} manifests itself by the occurrence of the shoulder at about 466 eV (B4). Such outstanding (and most importantly *spatially resolved*) sensitivity with respect to coordination of transition metals in glass tempted us to address the question whether or otherwise the titanium coordination in amorphised $Ba_2(TiO)(Si_2O_7)$ is different from that of the identically composed $2BaO-TiO_2-2SiO_2$ glass. Within a superficial layer, amorphization of $Ba_2(TiO)(Si_2O_7)$ can be readily achieved by bombarding it with accelerated rare-gas ions. In order to determine conditions under which complete amorphization is attained, the depth dependence of the minimum yield was determined from RBS channeling spectra of the perfect $Ba_2(TiO)(Si_2O_7)$ crystal and of the crystal irradiated with 200 keV Ar^+ ions at different fluences (Figure 2). Disregarding the surface peak, in the surface near region the minimum yield of the perfect $Ba_2(TiO)(Si_2O_7)$ crystal amounts to approximately 0.4, which is a relatively high value compared to the minimum yield measured in common single crystals such as silicon ($\chi_{min} < 0.05$). The high minimum yield of the perfect $Ba_2(TiO)(Si_2O_7)$ crystal is due to the dechanneling of the analyzing He ions at an incommensurate structural modulation hosted in the fresnoite framework structure.[16] On the average, such modulation has a similar effect as a strong thermal vibration of particularly oxygen ions about their average positions.

Irradiation with 200 keV Ar^+ ions at an ion fluence of $1 \cdot 10^{12}$ cm^{-2} provokes no changes of the minimum yield

(8) Höche, T.; Heyroth, F.; Grodzicki, M.; van Aken, P. A. *Phys. Status Solidi* **2005**, *202*, 2355−2360.
(9) Tesmer, J. R.; Nastasi, M.; Barbour, J. C.; Maggiore, C. J.; Mayer, J. W. *Handbook of Modern Ion Beam Materials Analysis*; Materials Research Society: Pittsburg, 1995.
(10) The CoatMaster tool for selective carbon coating is available through 3D-Micromac AG of Chemnitz, Germany (www. 3d-micromac.com).
(11) Höche, T.; Gerlach, J. W.; Petsch, T. *Ultramicroscopy*; doi: 10.1016/j.ultramic.2006.05.007.
(12) Strecker, A.; Salzberger, U.; Mayer, J. *Prakt. Metallogr.* **1993**, *30*, 482.
(13) van Aken, P. A.; Liebscher, B. *Phys. Chem. Miner.* **2002**, *29*, 188−200.
(14) Egerton, R. F. *Electron Energy-Loss Spectroscopy in the Electron Microscope*, 2nd ed.; Plenum Press: New York, 1996.
(15) Grodzicki, M.; *J. Phys B* **1980**, *13*, 2683−2691.
(16) Markgraf, S. A.; Halliyal, A.; Bhalla, A. S.; Newnham, R. E. *Ferroelectrics* **1985**, *62*, 17−26.

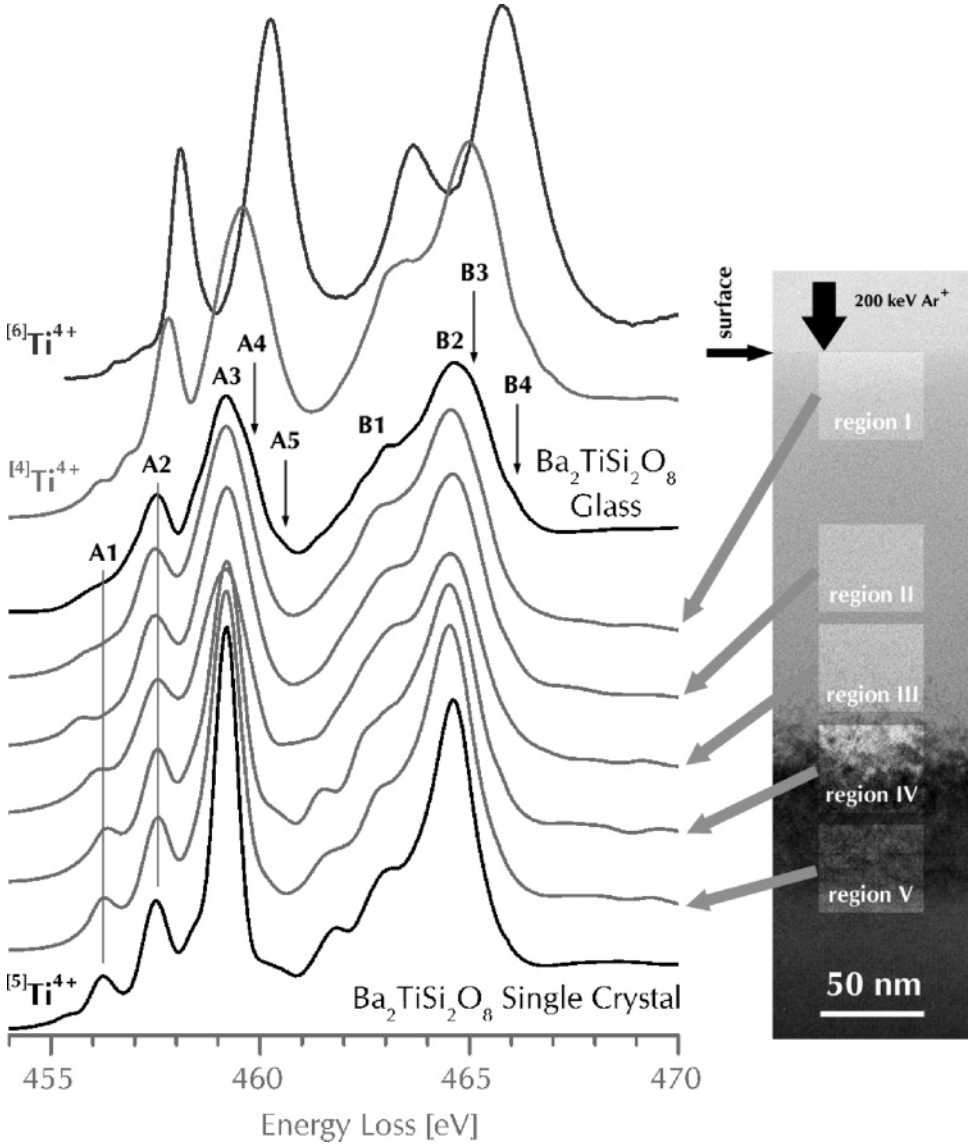

Figure 1. Ti-$L_{2,3}$ ELNES spectra acquired at different depths of the $Ba_2(TiO)(Si_2O_7)$ single crystal amorphized by Ar^+ irradiation in comparison to spectral reference data: tetrahedral coordination in β-Ba_2TiO_4; $^{[4]}Ti^{4+}$ (taken from ref 21), 5-fold (square-pyramidal) coordination found in fresnoite ($^5Ti^{4+}$), and octahedral coordination in $BaTiO_3$; $^6Ti^{4+}$ (taken from ref 21). Upon spectra acquisition, the electron beam was scanned across the areas indicated in the cross-sectional TEM image to minimize radiation damage. During ion irradiation, the Ar^+ beam came in from the top and provoked a medium gray amorphized layer ranging about 150 nm deep beneath the surface. This layer is succeeded by a "cloudy" transition region hosting crystalline fragments in an amorphous matrix. For comparison, the Ti-$L_{2,3}$ ELNES of single-crystalline $Ba_2(TiO)(Si_2O_7)$ and $2BaO-TiO_2-2SiO_2$ glass are also given. The integral intensity of all spectra was normalized between 455 and 467 eV, and the curves are plotted vertically staggered to facilitate their comparison.

(Figure 2). For an ion fluence of $1 \cdot 10^{13}$ cm^{-2}, a higher minimum yield is measured due to increased dechanneling of He ions on irradiation induced lattice defects. The minimum yield increases with increasing ion fluence and a damage peak at a depth slightly below 100 nm is observed, which is caused by the direct backscattering of He ions on lattice defects (i.e., a highly damaged layer is formed). The depth of the damage peak agrees very well with the distribution of displaced atoms calculated with the computer code SRIM (see Figure 2). After irradiation at an ion fluence of $1 \cdot 10^{14}$ cm^{-2}, the minimum yield reaches the value of unity which is, according to RBS, equal to complete amorphization. At the latter fluence, a superficial amorphous layer of approximately 100 nm thickness is formed. Below this layer and down to a depth of 250 nm, the initially single-crystalline $Ba_2(TiO)(Si_2O_7)$ is strongly modified but not entirely amorphous. These results, however, only reflect the degree of damage as related to the dechanneling of He^+ ions and does not allow direct conclusions with respect to the type of structural modification.

The latter modification can also not become resolved by imaging the Ar^+ irradiated $Ba_2(TiO)(Si_2O_7)$ single crystal in a transmission electron microscope. However, in the cross-sectional TEM micrograph (Figure 1), a modified superficial layer totally extending to 260 nm depth into the crystal is found. At the lower end of the modified layer, a ~55 nm thick region V can be discerned that is not amorphized, and point defects are most likely responsible for the dechanneling evident in the RBS spectrum. This region is covered by the ~55 nm thick region IV, in which crystalline fragments are embedded into an amorphous matrix. Between the surface and the top of region IV (depth $\approx$ 150 nm), the $Ba_2(TiO)(Si_2O_7)$ single crystal appears to be completely amorphized. Since minor fractions of crystalline clusters in an amorphous

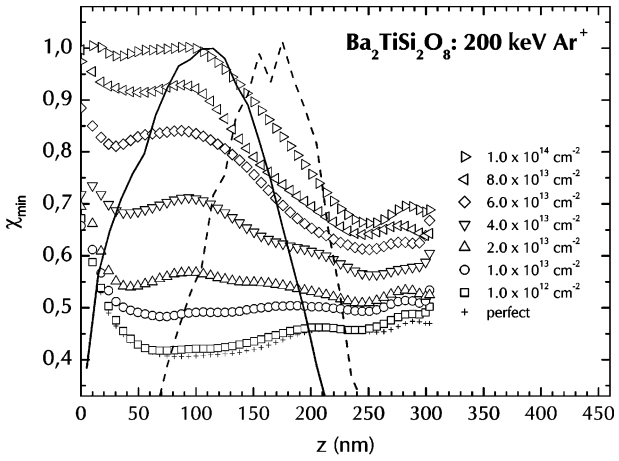

Figure 2. Smoothed minimum yield, χ_{min}, as a function of depth, *z*, obtained from RBS channeling spectra of a $Ba_2(TiO)(Si_2O_7)$ single-crystal irradiated with 200 keV Ar^+ ions at different ion fluences. Additionally, the calculated distributions of displaced lattice atoms (solid line) and implanted Ar ions (dashed line) are given in arbitrary units.

ambient cannot be resolved by high-resolution TEM,[17] it is not astonishing that the RBS measurement did indicate incomplete amorphization in the depth range between 100 and 150 nm. ELNES spectroscopy was hence applied at different depths to resolve this apparent discrepancy. As shown in Figure 1, ELNES spectra acquired from a scanning area of 40 × 50 nm^2 in depths of 0−40 nm (region I), 80−120 nm (region II), and 130−170 nm (region III), respectively, in fact possess very significant differences.

From the juxtaposition of the Ti-$L_{2,3}$ ELNES spectrum of amorphized $Ba_2(TiO)(Si_2O_7)$ taken from region I and the $2BaO-TiO_2-2SiO_2$ glass (Figure 1), it becomes apparent that the amorphized layer can—due to the characteristic shape of the corresponding Ti-$L_{2,3}$ ELNES—unambiguously be assigned to the presence of $^{[5]}Ti^{4+}$. Detailed inspection, however, reveals that minima and maxima of the amorphized $Ba_2(TiO)(Si_2O_7)$ Ti-$L_{2,3}$ ELNES are even more pronounced than the corresponding features in the $2BaO-TiO_2-2SiO_2$ glass Ti-$L_{2,3}$ ELNES, and the width of the peaks is smaller than in the glass. Moreover, maxima in the Ti-L_3 ELNES of amorphized $Ba_2(TiO)(Si_2O_7)$ in region I (especially peak A3 at 459.1 eV, assigned to the Ti-$3d_z^2$ orbital) possess a much higher peak-shape symmetry than the corresponding spectral features in the glass Ti-L_3 ELNES. This observation is strongly indicative of primarily pentahedrally coordinated Ti^{4+} at this depth. As discussed earlier, tetrahedrally co-ordinated Ti^{4+} is giving rise to peaks A4 and B3 indicated in Figure 1, while octahedrally co-ordinated Ti^{4+} causes the occurrence of peaks A5 and B4. Such peaks cannot be discerned in the amorphised single crystal, the contribution of non-pentahedrally co-ordinated Ti^{4+} (20% $^{[4]}Ti^{4+}$ plus 20% $^{[6]}Ti^{4+}$ in $2BaO-TiO_2-2SiO_2$ glass of identical composition[3]) must therefore be significantly smaller if ever present in the amorphised single crystal.

A different picture arises in regions II and III of the irradiated $Ba_2(TiO)(Si_2O_7)$ single crystal. Besides a pronounced peak broadening in comparison to the spectra from regions IV and V being related to the absence of crystalline fragments (cf. Figure 1), the major deviation is found for peak A1. This peak is related to the Ti($3d_{xy}$) orbital[3] and significantly shifted toward lower energy losses in regions II and III. Recent theoretical studies[18] have shown that the position of this peak is closely related to the bond length between the titanium ion inside the square pyramid and the apical oxygen ion (O4) such that a lowering of the bond length causes a shift of the peak toward lower energy losses. Hence, the Ti-$L_{2,3}$ ELNES spectra acquired at regions II and III are consistent with a nanoscopic picture comprising large argon atoms squeezed into the amorphous network at depths where they become deposited (see Ar distribution in Figure 2). The latter atoms provoke locally enhanced compressive stresses leading to very significant distortions of the coordination polyhedra and—on the average—shorter bond length. The bond lengths distribution is thus found to be much wider than both in the single crystal and at depths within the amorphised crystal where no argon is deposited.

Conclusion

Depth-dependent changes of the transition-metal coordination in a superficially amorphized single crystal were profiled by high-resolution ELNES spectroscopy for the first time. The interpretation of the spectra (particularly in larger depths) is consistent with the build-up of high internal stresses. Such spatially resolved experimental assess to transition-metal coordination is of great importance for (in-situ) studies at recrystallization and crystallization phenomena in amorphous matter (e.g., relevant for the fabrication of buried refractive index barriers in waveguides).[19,20] It will moreover be very useful for investigating the atomistic structure of amorphous grain-boundary thin films in sintered ceramics as well as the network structure of ultrathin gate dielectrics in integrate circuits.

Acknowledgment. Growth of the $Ba_2(TiO)(Si_2O_7)$ single crystal by R. Uecker (Institut für Kristallzüchtung Berlin), preparation of the $2BaO-TiO_2-2SiO_2$ glass by R. Keding (Institut für Glaschemie, Friedrich-Schiller-Universität Jena), computing time provided by RIST (Universität Salzburg), and granted access to the high-resolution TEM facilities at the MPI for Microstructure Physics Halle by U. M. Gösele are gratefully acknowledged.

CM060636A

(17) Miller, M. L.; Ewing, R. C. *Ultramicroscopy* **1993**, *48*, 203−237.
(18) Höche, T.; Grodzicki, M.; Heyroth, F.; Uecker, R.; van Aken, P. A. *Philos. Mag. Lett.* (submitted for publication).
(19) Schrempel, F.; Höche, T.; Ruske, J. P.; Grusemann, U.; Wesch, W. *Nucl. Instrum. Methods B* **2002**, *191*, 202−207.
(20) Höche, T.; Kleebe, H. J.; Schrempel, F.; Wesch, W. *Philos. Mag. Lett.* **2002**, *82*, 599−608.